Response Control by Damper Tube System utilizing Torsional Vibration

H. Kurino & N. Kano
Kajima Corporation, Japan

SUMMARY:
This paper proposes a new vibration control system that realizes substantial earthquake response reduction utilizing torsional vibration. It consists of an eccentric core structure, perimeter frames with pin-joint post-columns that support only the vertical load, slab elements that transmit shear force between the core structure and the perimeter frames, and energy dissipation devices (dampers) installed in the perimeter frames. The dampers effectively absorb vibration energy by utilizing torsional vibration, which is usually avoided in seismic design. The system is nicknamed "Damper Tube Structure". The control effect and the damper requirements including the optimum damper distribution problem are discussed using a simple one-axis eccentric mathematical model based on the CQC method and the viewpoint of energy balance. To examine the effectiveness of the proposed simple design flow, earthquake response analyses with a two-axis eccentric model are conducted, and promising results that indicate the potential of the system are obtained.

Keywords: Structural Control, Torsional Vibration, Energy Absorption, Oil Damper, Robustness

1. INTRODUCTION

This paper proposes a new structural control system that realizes substantial earthquake response reduction utilizing torsional vibration. It consists of an eccentric core structure, flexible perimeter frames with pin-jointed post-columns that support only vertical loads, slab elements that transmit shear force between the core structure and the perimeter frames, and energy dissipation devices (dampers) installed in the perimeter frames diagonally like a net. Inputted seismic energy is converted into torsional vibration energy due to the eccentricity of the core structure, and the dampers arranged in the perimeter frames effectively resist and absorb the energy utilizing torsional vibration, which is usually avoided in seismic design. The system is nicknamed "Damper Tube Structure (DTS)". It should be mentioned that fluctuation of seismic response against unexpected change of eccentricity is small because when the perimeter frames' displacements become larger due to torsional vibration, the efficiency of the damper increases. This mechanism gives the structure robustness and redundancy against fluctuation of design parameters and disturbances. Moreover, the deformation of the core structure can be kept small because of the feature of torsional vibration, and because the perimeter frames are pin-jointed flexible structures, a building with no damage can be easily realized even in severe earthquakes. In addition to these attractive features from the viewpoint of seismic design, there is a possibility of realizing a new architectural design in countries like Japan that are subject to severe earthquakes because the arrangement of the core structure is free and connections of other frames and slab elements can be pin-jointed.

This paper first outlines the concept and components of this system, and then discusses the control principle, the effects and the damper requirements including the optimum damper distribution problem using a simple one-story one-axis eccentric mathematical model based on the CQC (Complete Quadratic Combination) method. Then, we propose a simple design flow including how to deal with a two-axis eccentric system, and demonstrate the earthquake response analysis results using a two-axis eccentric vibration model.

2. CONSTITUTION OF DAMPER TUBE STRUCTURE

The concept of the Damper Tube Structure (DTS) is "a structure of free-planning, low-stiffness and greatly response controlled". In this system, though the core structure is the only stiffness element that resists static horizontal load, its arrangement in the plan is permitted to be free to ensure high planning flexibility. The other frames, including the perimeter frames, are designed as flexible structures such as pin-jointed post-columns that support only vertical loads. Compared with conventional seismically designed structures, the DTS has low stiffness and large eccentricity because the stiffness element is only the core structure, and its arrangement is permitted to be free. Thus, we introduce energy dissipation devices (dampers) into the perimeter frames diagonally like a net to control horizontal, torsional and vertical vibration. The slab of each floor is an important structural element that transmits shear force between the core structure and the perimeter frames. Fig. 1 shows a conceptual diagram of the DTS.

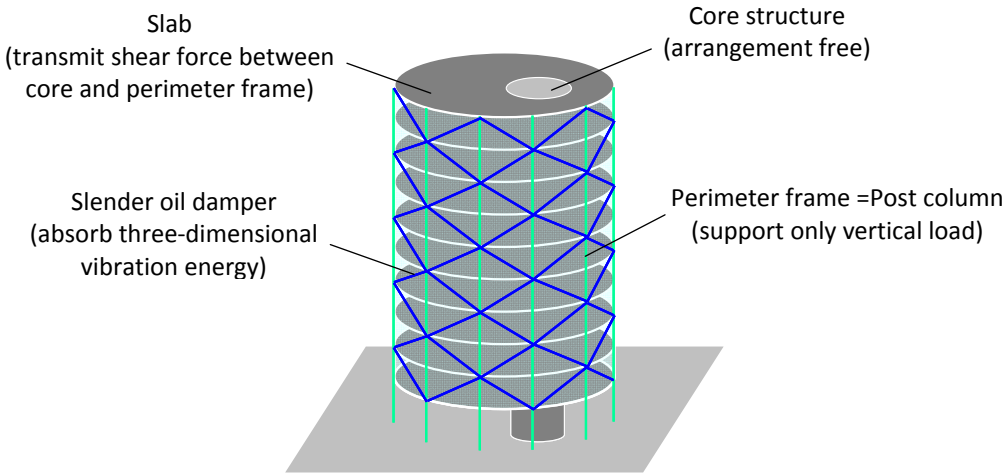

Figure 1. Conceptual diagram of Damper Tube Structure

3. FUNDAMENTAL STUDY ON ONE-STORY ONE-AXIS ECCENTRIC MODEL

3.1. Target Vibration Model and Fundamental Vibration Characteristics

A typical plan of the model structure is shown in Fig. 2(a), and Fig. 2(b) represents its simplified one-story one-axis eccentric vibration model. In Fig. 2(b), G represents the centre of gravity, S represents the centre of stiffness and D is the centre of the dampers arranged in the perimeter frames at $x=\pm a/2$ and $y=\pm b/2$. C_x and C_y are the damper's total damping coefficients in the X and Y directions, respectively, and α expresses the distribution ratio of C_y to the right and left sides.

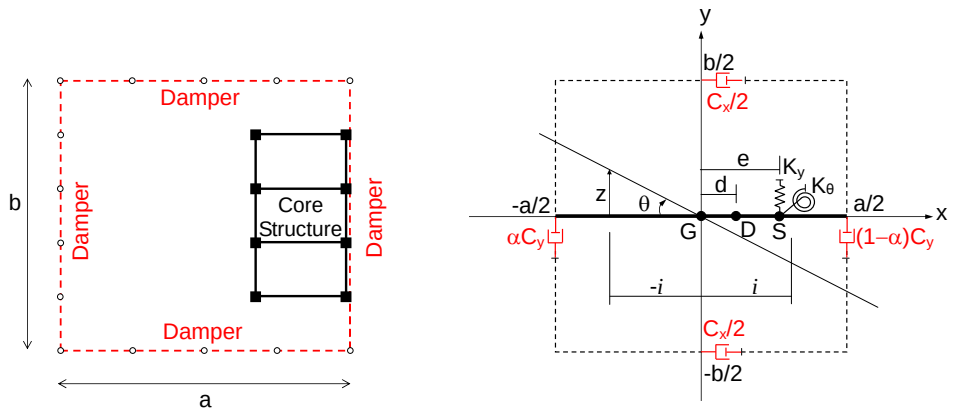

(a) Plan of model building (b) One-axis vibration model

Figure 2. One-axis eccentric vibration model

If we neglect the internal structural damping, the equation of motion of this system with ground acceleration $\ddot{y}_g$ for Y direction is expressed:

$$\begin{bmatrix} m & \\ & I \end{bmatrix}\begin{Bmatrix} \ddot{y} \\ \ddot{\theta} \end{Bmatrix}+\begin{bmatrix} C_y & -dC_y \\ -dC_y & d^2C_y+C_\theta \end{bmatrix}\begin{Bmatrix} \dot{y} \\ \dot{\theta} \end{Bmatrix}+\begin{bmatrix} K_y & -eK_y \\ -eK_y & e^2K_y+K_\theta \end{bmatrix}\begin{Bmatrix} y \\ \theta \end{Bmatrix}=-\begin{bmatrix} m & \\ & I \end{bmatrix}\begin{Bmatrix} 1 \\ 0 \end{Bmatrix}\ddot{y}_g \tag{3.1}$$

where m is mass, I is rotational inertia, K_y is core structure stiffness in Y direction, K_θ is core structure torsinonal stiffness around S, and e is eccentricity. d (damping eccentricity) and C_θ (torsional damping coefficient around D) are expressed by:

$$d=(1-2\alpha)a/2 \tag{3.2}$$

$$C_\theta=\alpha(1-\alpha)a^2C_y+(b^2/4)C_x \tag{3.3}$$

Here, we replace parameters $I/m=i^2$, $K_y/m=\omega_y{}^2$, $C_y/m=2h_y\omega_y$, $C_\theta/C_y=r^2$ and $K_\theta/K_y=j^2$, and introduce non-dimensional parameters $e/i=\bar{e}$, $j/i=\bar{j}$, $d/i=\bar{d}$, $r/i=\bar{r}$. If we express the rotation angle θ in terms of displacement at radius of gyrarion ($x=\pm i$) as $\theta=z/i$ as shown in Fig.2(b), Eqn. 3.1 can be rewritten as:

$$\begin{bmatrix} 1 & \\ & 1 \end{bmatrix}\begin{Bmatrix} \ddot{y} \\ \ddot{z} \end{Bmatrix}+2h_y\omega_y\begin{bmatrix} 1 & -\bar{d} \\ -\bar{d} & \bar{d}^2+\bar{r}^2 \end{bmatrix}\begin{Bmatrix} \dot{y} \\ \dot{z} \end{Bmatrix}+\omega_y{}^2\begin{bmatrix} 1 & -\bar{e} \\ -\bar{e} & \bar{e}^2+\bar{j}^2 \end{bmatrix}\begin{Bmatrix} y \\ z \end{Bmatrix}=\begin{Bmatrix} -\ddot{y}_g \\ 0 \end{Bmatrix} \tag{3.4}$$

where spring radius ratio $\bar{j}$ is a very important parameter in the torsional vibration problem. As is well known, the relationship between the 1st mode and the 2nd mode of the one-axis eccentric model changes drastically at around $\bar{j}=1$. Because the core structure is the only stiffness element in this system and the core area is several times smaller than the floor area, spring radius j must be smaller than the radius of gyration i, i.e.:

$$\bar{j}\le 1 \tag{3.5}$$

We should pay attention to Eqn. 3.5 when considering the dynamic characteristics of this system.

Suppose $\{y, z\}^{\mathrm{T}}=\{u, w\}^{\mathrm{T}}e^{i\omega t}$ and substituting this into Eqn. 3.4 and introducing $\omega/\omega_y=\lambda$, the no-damping equations of motion can be solved in a closed form, and the eigenvalues and the eigen vectors are expressed as:

$$\lambda^2=\frac{1+\bar{e}^2+\bar{j}^2\pm\sqrt{(1+\bar{e}^2+\bar{j}^2)^2-4\bar{j}^2}}{2} \tag{3.6}$$

$$\begin{Bmatrix} u \\ w \end{Bmatrix}=\begin{Bmatrix} 1 \\ (1-\lambda^2)/\bar{e} \end{Bmatrix} \tag{3.7}$$

The participation factor for Y-direction ground acceleration is expressed as:

$$\beta=\begin{Bmatrix} u \\ w \end{Bmatrix}^T\begin{bmatrix} 1 & \\ & 1 \end{bmatrix}\begin{Bmatrix} 1 \\ 0 \end{Bmatrix}\Bigg/\begin{Bmatrix} u \\ w \end{Bmatrix}^T\begin{bmatrix} 1 & \\ & 1 \end{bmatrix}\begin{Bmatrix} u \\ w \end{Bmatrix}=\frac{\bar{e}^2}{\bar{e}^2+(1-\lambda^2)^2} \tag{3.8}$$

Fig. 3 shows the relationship between the eccentricity ratio $\bar{e}$ and the dynamic characteristics for various spring radius ratios. Fig. 3(a) shows the ratio of the eigen period T to T_y which is the natural period for translation with no eccentricity, (b) shows the participation function βu at $x=-i$ (soft side), and (c) shows the participation function βu at $x=i$ (stiff side). As mentioned above, relationship between the 1st mode and the 2nd mode changes drastically at around $\bar{j}=1$, but when the eccentricity ratio $\bar{e}$ becomes large, βu tends to converge.

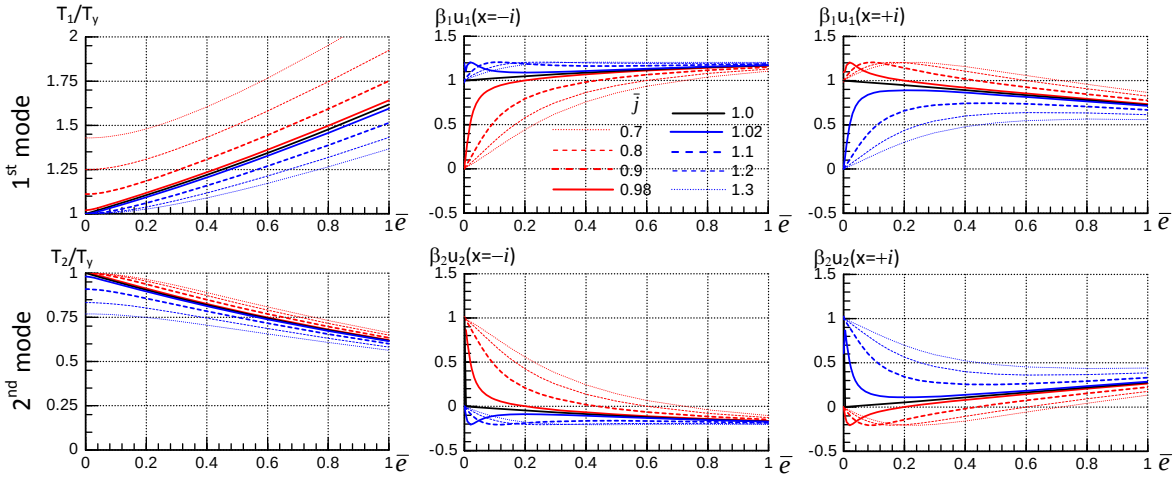

(a) Change of period T/T_y (b) Participation function βu at x=-i (c) Participation function βu at x=i

Figure 3. Dynamic characteristic of one-axis eccentric vibration model

Next, we examine the system modal damping ratio realized by the dampers arranged in the perimeter frames. Since the damping matrix of this system is non-proportional to the mass and stiffness matrices, complex eigenvalue analysis is required to accurately evaluate the damping ratio, but here we try to estimate it by an approximate method using a diagonal element of the modal damping matrix using eigenvalues and eigenvectors of the no-damping system. System modal damping ratio h_D realized by the dampers is expressed as:

$$h_D = \frac{\overline{C}}{2\omega\overline{M}} = \frac{(1-\bar{d}\bar{\phi})^2 + \bar{r}^2\bar{\phi}^2}{\lambda\left(1+\bar{\phi}^2\right)} h_y \tag{3.9}$$

where $\overline{M} = \begin{Bmatrix} u \\ w \end{Bmatrix}^T \begin{bmatrix} 1 & \\ & 1 \end{bmatrix} \begin{Bmatrix} u \\ w \end{Bmatrix}$, $\overline{C} = 2h_y\omega_y \begin{Bmatrix} u \\ w \end{Bmatrix}^T \begin{bmatrix} 1 & -\bar{d} \\ -\bar{d} & \bar{d}^2+\bar{r}^2 \end{bmatrix} \begin{Bmatrix} u \\ w \end{Bmatrix}$, $\bar{\phi} = \dfrac{1-\lambda^2}{\bar{e}}$

Fig. 4 shows the change of modal damping ratio h_D according to the change of eccentricity ratio $\bar{e}$, where the side length ratio is b/a=1, and the total damping coefficient C_x and C_y for the X and Y directions are set as h_x=h_y=0.05. Results for three different damping distribution ratio α are shown in Fig. 4, and (a) is the case for α=0 (C_y is placed intensively at x=a/2), (b) is the case for α=0.5 (C_y is distributed to x=$\pm a$ evenly), (c) is the case for α=1.0 (C_y is placed intensively at x=-a/2). The augmented damping ratio when the eccentricity is large is influenced by the damper distribution ratio α, and we can recognize the difference of the spring radius ratio $\bar{j}$ in the 1st mode but there is no significant difference in the 2nd mode. When the eccentricity ratio $\bar{e}$ becomes larger than 0.3～0.4, the fluctuation of modal damping ratio becomes very small. For reference, some damping ratios obtained by the complex eigevalue analysis are also shown in Fig. 4, and it is confirmed that the approximate method employed here is sufficient for the scope of this study.

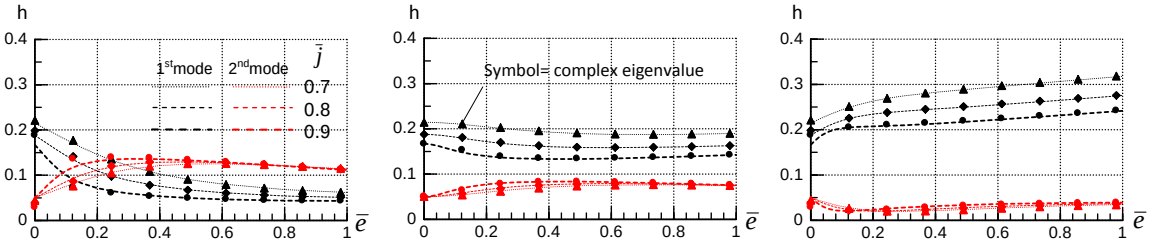

(a) α=0 (b) α=0.5 (c) α=1.0

Figure 4. System modal damping ratio (b/a=1, h_0=0, h_x=h_y=0.05)

3.2. Damper Requirements

We assume that the relationship between the maximum earthquake response value R and the building's damping ratio h can be expressed by:

$$R \propto \frac{1}{\sqrt{1+Nh}} \tag{3.10}$$

where h in Eqn. 3.10 represents the sum of structural internal damping h_0 and the augmented damping ratio h_D by the dampers. N is a coefficient that indicates damping sensitivity, and is determined by the earthquake's characteristic (duration). The observed records with short duration and simulated earthquakes with long duration show that the value of N is approximately 25 to 50. If we assume that the velocity spectrum is almost constant in the range of the target building's vibration period, the ratio of the response displacement δ of an eccentricity model to that of a no-eccentricity model (e=0) can be expressed by:

$$\frac{\delta}{\delta_y} = \sqrt{\frac{1+N(h_0+h_y)}{1+N(h_0+h_D)}}\,\frac{\omega_y}{\omega} \tag{3.11}$$

where δ_y, h_y, ω_y are displacement response, augmented damping ratio by dampers and circular frequency for no eccentricity (e=0), respectively.

Here we examine the required damping ratio on condition that the response displacement of no eccentricity (e=0) should be equivalent to that of a conventional seismically designed structure. Because the core structure is the only stiffness element in the DTS, the natural period becomes longer than that of a conventional seismically designed structure. From the design examples, the stiffness of the DTS is almost half that of the a conventional seismically designed structure (=frequency is almost $1/\sqrt{2}$ times), and the required damping ratio h_D for no eccentricity is determined by:

$$\frac{1}{\sqrt{1+Nh_0}} = \frac{1}{\sqrt{1+N(h_0+h_D)}} \times \sqrt{2} \tag{3.12}$$

Transforming Eqn. 3.12, we obtain:

$$h_D = h_0 + \frac{1}{N} \tag{3.13}$$

Evaluated h_D is about 0.04~0.06 for the condition of N=25~50 and h_0=0.02, and is realizable by oil dampers with good performance.

3.3. Estimation of Earthquake Response by CQC Method

Considering the participation function value at evaluation point based on the relationship shown in Eqn. 3.11, we estimate the ratio of response displacement of the eccentric model ($\bar{e} \neq 0$) to the no-eccentricity (translation) model. Here we adopt the CQC (Complete Quadratic Combination) method for superposition of the 1st mode response δ_1 and the 2nd mode response δ_2 considering the period's proximity and the large damping ratios. Maximum response value $\delta_{\max}$ is expressed by δ_1, δ_2 and modal correlation coefficient ρ_{12} as:

$$\delta_{\max} = \sqrt{\delta_1^{\,2} + 2\rho_{12}\delta_1\delta_2 + \delta_2^{\,2}} \tag{3.14}$$

$$\rho_{12} = \frac{8\sqrt{h_1 h_2}\,(h_1 + q h_2)\,q^{1.5}}{(1-q^2)^2 + 4h_1 h_2 q(1+q^2) + 4(h_1^{\,2} + h_2^{\,2})q^2}, \qquad q = \frac{\omega_2}{\omega_1} \tag{3.15}$$

Fig. 5 shows an example of the estimated response displacement at various evaluation points for various radius spring ratios (but $\bar{j} \leq 1$) using the three models with the ratios of side length b/a=0.5, 1,

2 (a=1). The horizontal axis shows eccentricity e as well as eccentricity ratio $\bar{e}$, the vertical axis shows the estimated response displacement normalized by the displacement for the no-eccentricity case. We set N=35, h_0=0.02, h_x=h_y=0.05 and the damper distribution ratio α=0.5 (equal on both sides). The Y-direction displacement at the centre of stiffness S (x=e) which represents response shear force, the Y-direction displacement at $x=\pm a/2$ (=perimeter frame's displacement), and the X-direction displacement at $y=\pm b/2$ (=orthogonal perimeter frame's displacement) are indicated in the figure. This is a typical feature of the condition $\bar{j} \le 1$. The stiff side displacement (x=a/2) is larger than the soft side displacement (x=-a/2) when the eccentricity ratio $\bar{e}$ is small, but the soft side displacement becomes larger when the eccentricity ratio $\bar{e}$ becomes larger than about 0.4. The displacement at the centre of stiffness (=shear force) decreases with increase in eccentricity, reaching about 60~70 % of the no-eccentricity case when $\bar{e}$ is larger than about 0.4.

Fig. 6 shows the effect of damper distribution ratio α. Fig. 6(b) is identical to Fig. 5(b), but Figs. 6(a) and (c) show the cases of α=0 (concentrated on stiff side) and α=1 (concentrated on soft side), respectively. Focusing on the response control of perimeter frame displacement, the figures imply that there is an optimum damper distribution ratio α_{opt} according to the eccentricity ratio $\bar{e}$. On the other hand, the response at the centre of stiffness (shear force) does not depend on α, and decreases with increase in $\bar{e}$.

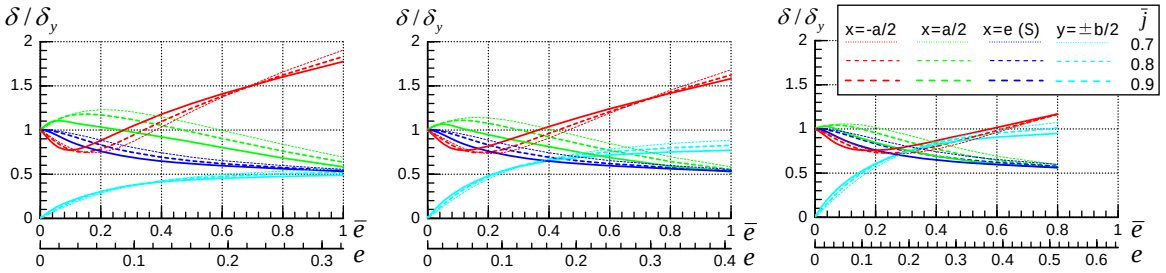

(a) a=1, b=0.5 (b) a=1, b=1 (c) a=1, b=2

Figure 5. Change of response displacement (h_0=0.02, h_x=h_y=0.05, α=0.5, N=35)

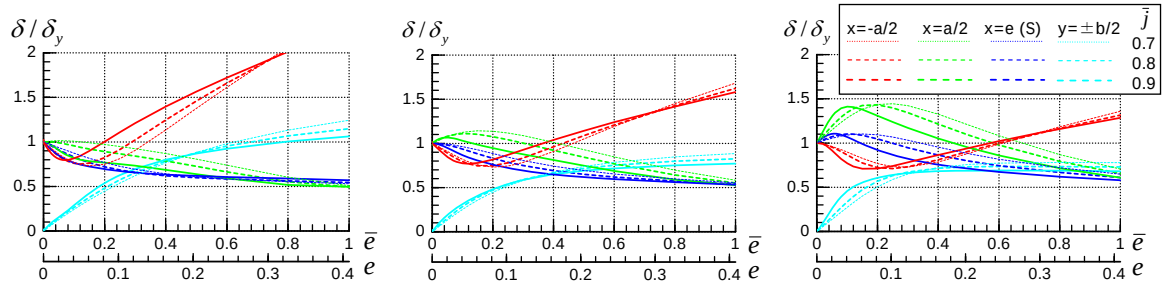

(a) α=0 (b) α=0.5 (c) α=1

Figure 6. Effect of damper distribution ratio α (a=b=1, h_0=0.02, h_x=h_y=0.05, N=35)

3.4. Consideration of Response Reduction Principle from a Viewpoint of Energy Balance

Here we consider the mechanism of the response displacement at the centre of stiffness (shear force) reducing when there is large eccentricity from the viewpoint of energy balance. Each mode's effective mass for Y-direction ground motion is expressed by:

$$\overline{m} = \left(\begin{Bmatrix} u \\ w/i \end{Bmatrix}^T \begin{bmatrix} m & \\ & I \end{bmatrix} \begin{Bmatrix} 1 \\ 0 \end{Bmatrix} \right)^2 \Bigg/ \begin{Bmatrix} u \\ w/i \end{Bmatrix}^T \begin{bmatrix} m & \\ & I \end{bmatrix} \begin{Bmatrix} u \\ w/i \end{Bmatrix} = \frac{\bar{e}^2 m}{\bar{e}^2 + (1-\lambda^2)^2} = \beta m \tag{3.16}$$

Eqn. 3.16 indicates that the rotational inertia I and eccentricity e do not influence the sum of effective masses because $\Sigma\beta$=1. Therefore, if we assume that the vibration period of the target building is included in the period range where the velocity spectrum (or energy spectrum) is constant, the total

energy inputted into a two-degree-of-freedom system with eccentricity ($e \neq 0$) is equivalent to that inputted into a single-degree-of-freedom system without eccentricity ($e=0$). Energy inputted into each mode in proportion to the effective mass is converted into translation and rotational direction potential energy, and the greater the conversion to rotational direction, the lesser the translation potential energy (translation displacement). If we put E_s as translation potential energy and E_r as rotational potential energy, their ratio for each mode is expressed by:

$$E_s : E_r = \lambda^4 : \bar{j}^2 \left(\frac{1-\lambda^2}{\bar{e}} \right)^2 \tag{3.17}$$

Fig. 7(a) shows an example of energy distribution for $\bar{j} = 0.8$. As can be seen from the figure, the ratio of conversion into rotational potential energy becomes large when eccentricity ratio $\bar{e}$ becomes large, and reaches about 50% when $e \geq 0.3 \sim 0.4$. In addition, the energy absorption efficiency for rotational direction is far larger than that for translation direction in the DTS, so these features realize excellent response reduction of translational displacement (=shear force). Fig. 7(b) explains the relationship between the response displacement and the change of modal vibration characteristics due to the reduction of structural stiffness, introduction of an eccentricity and addition of damping, by using an explanatory displacement response spectrum for b/a=1, $\bar{j} = 0.8$, h_0=0.02, h_x= h_y=0.05, α=0.5, and N=35. We can thus comprehend how the response is reduced by the DTS from the diagram.

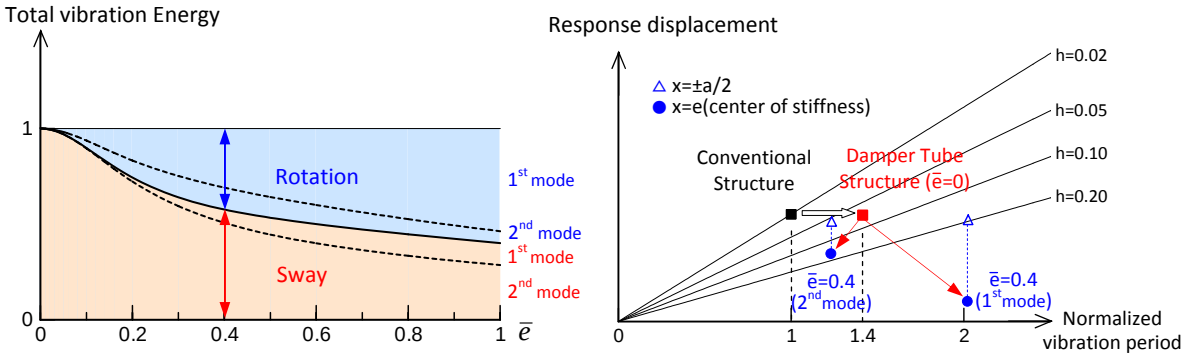

(a) Eccentricity and energy distribution (b) Change of modal characteristic and response displacement

Figure 7. Conceptual diagrams explaining how response reduces with eccentricity

3.5. Optimum Damper Distribution

This chapter discusses the optimum damper distribution. The problem is to find the required total damping coefficient C_y and the optimum damper distribution ratio α_{opt} that keeps the perimeter frame's Y-direction response displacement within its X-direction displacement (=no-eccentricity direction). Instead of C_y, here we use h_y, which expresses the damping ratio when e=0. Fig. 8 shows the required minimum damping ratio h_{ymin} and the optimum damper distribution ratio α_{opt}, examined on condition of h_0=0.02, h_x=0.05, and N=35. The results show that both h_{ymin} and α_{opt} depend on side length ratio b/a, and it is reasonable to choose $\alpha \to 0$ when $\bar{e}$ is small, and $\alpha \to 1$ when $\bar{e}$ becomes large. For h_{ymin}, it is understood that h_{ymin} is not always larger than h_x, and there are special conditions where h_{ymin} can be 0. This is because the dampers in the orthogonal frames work effectively when the side length ratio of the plan b/a is large, and it is possible to face this situation in an actual design process.

The above results shown in Fig. 8 are very interesting but here we introduce an additional condition of $h_{ymin} \geq h_x$ (=damping ratio of no-eccentricity direction) to leave a margin for parameter fluctuation under actual conditions. Fig. 9 shows the examination results for h_0=0.02, h_x=0.05, $h_{ymin} \geq h_x$=0.05, and N=35. The required damping ratio h_{ymin} and the optimum damper distribution ratio α_{opt} under the new condition are shown in the first row and the second row, respectively. Because the condition $h_{ymin} \geq h_x$ is introduced, α_{opt} has a range. h_{ymin} and α_{opt} can be approximated by following simple formula:

$$h_{y\min} = 0.1\bar{e} + 0.03(1 - b/a) \qquad \left(h_{y\min} \geq h_x\right) \tag{3.18}$$

$$\alpha_{opt} = 2\bar{e} + 2\bar{j} - 1.8 \qquad \left(0 \leq \alpha_{opt} \leq 1\right) \tag{3.19}$$

Since it is natural to set α=0.5 when e=0, and considering the difference of the control effect by α when e is small, it seems reasonable to introduce an additional condition $\alpha_{opt} \geq 0.5$ to Eqn. 3.19. The third row of Fig. 9 shows the total Y-direction damper force F_{ytotal} normalized by the damper force when e=0. Even if we boldly adopt very large eccentricity, the perimeter frame's displacement can be controlled within the permissible range without greatly increasing the number of dampers.

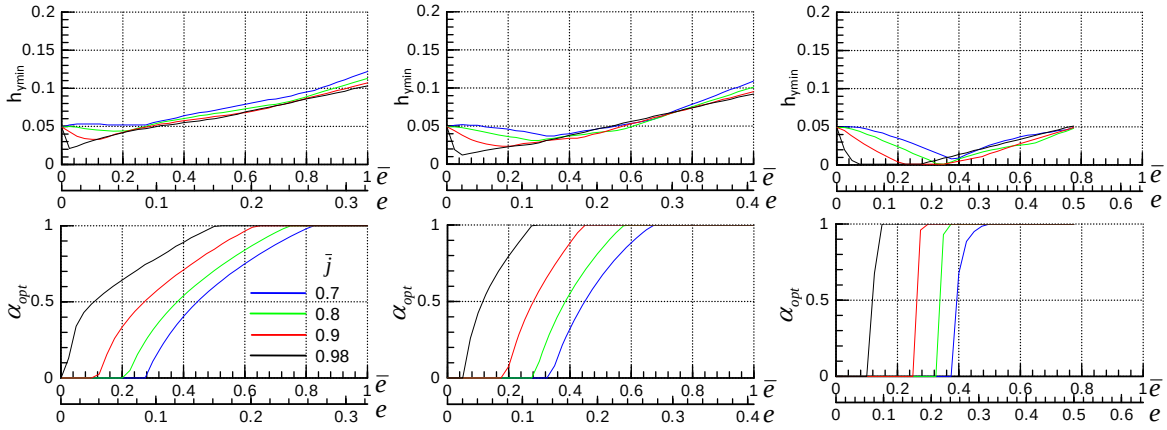

(a) a=1, b=0.5 (b) a=1, b=1 (c) a=1, b=2

Figure 8. Damper requirements (h_0=0.02, h_x=0.05, $h_y \geq 0$, N=35)

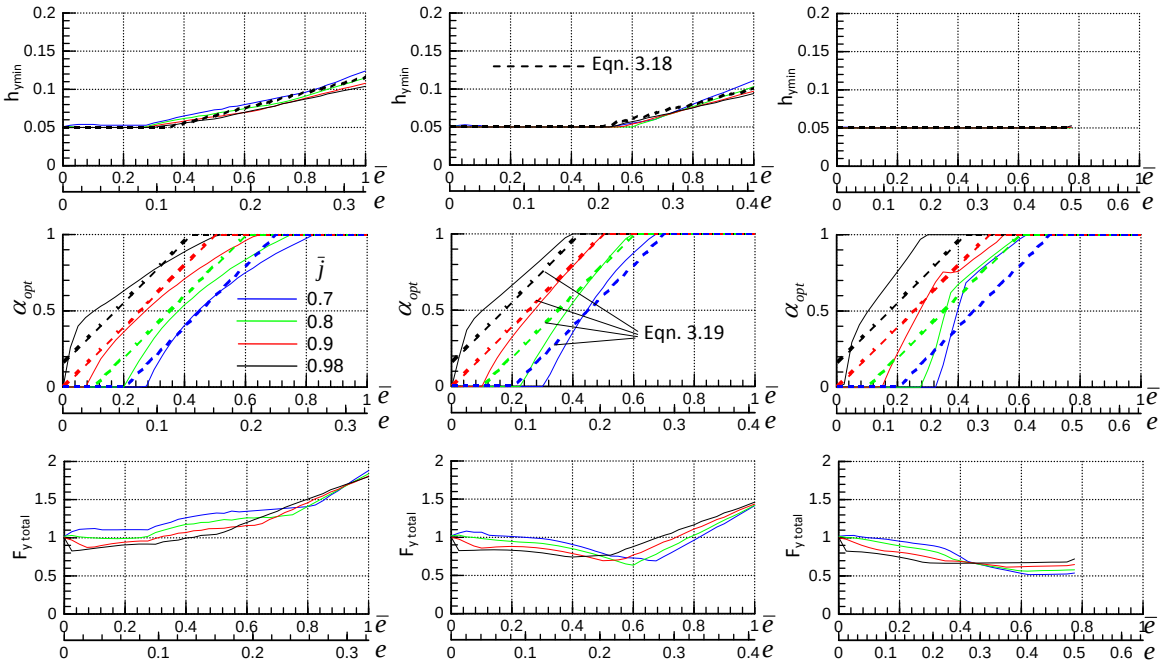

(a) a=1, b=0.5 (b) a=1, b=1 (c) a=1, b=2

Figure 9. Damper requirements (h_0=0.02, h_x=0.05, $h_y \geq h_x$, N=35)

4. EARTHQUAKE RESPONSE ANALYSIS

4.1. Design Flow for Two-Axis Eccentric Building

Based on the study in the previous section, we summarize the design flow of the DTS as:

(1) Design frames except core structure considering only vertical load.

(2) Set target period for no-eccentricity as $\sqrt{2}$ times that for a conventional structure.

(3) Design core structure according to target stiffness set in step (2).
(4) Evaluate eccentricity ratios $\bar{e}_x$, $\bar{e}_y$ and spring radius ratios $\bar{j}_x$, $\bar{j}_y$ by eigenvalue analysis.
(5) Estimate $h_{\min}$ and α_{opt} from Eqns. 3.18 and 3.19 for each direction (but $h_{\min} \geq 0.05$, $\alpha_{opt} \geq 0.5$).
(6) Arrange dampers in perimeter frames and conduct earthquake response analysis.

4.2. Earthquake Response Analysis using Two-axis Eccentric Model

To assess the effectiveness of the above design method, we conducted earthquake response analyses using a one-story two-axis eccentric vibration model. Fig. 10 shows the plan of the model, and seven different locations of the centre of stiffness were selected as indicated in the figure. The translational period was set to 2.0 seconds. Eccentricity ratios and damper conditions are summarized in Table 1. Three simulated earthquakes set up for usual seismic design in Japan were selected here, and their time histories and velocity spectrums are shown in Fig. 11. Approximate values of N are also indicated in the figure. A 45 degree earthquake direction is selected in addition to the X and Y directions as shown in Fig. 10. In addition to cases (1)~(7), we also set up a model representing a conventional seismically designed structure named case (0) for comparison, with a vibration period and a damping ratio of T=1.4 seconds and h_0=0.02, respectively.

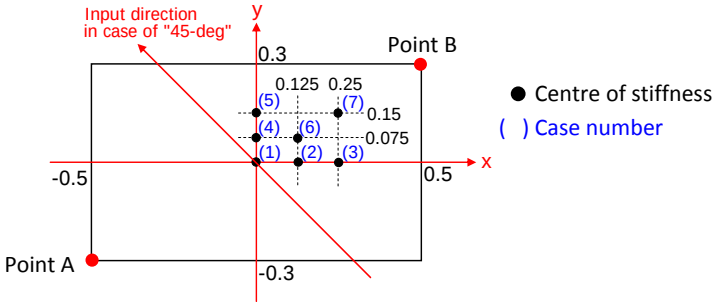

Figure 10. Two-axis eccentric vibration model (T_x=T_y=2.0 second, $\bar{j} = 0.8$, h_0=0.02,)

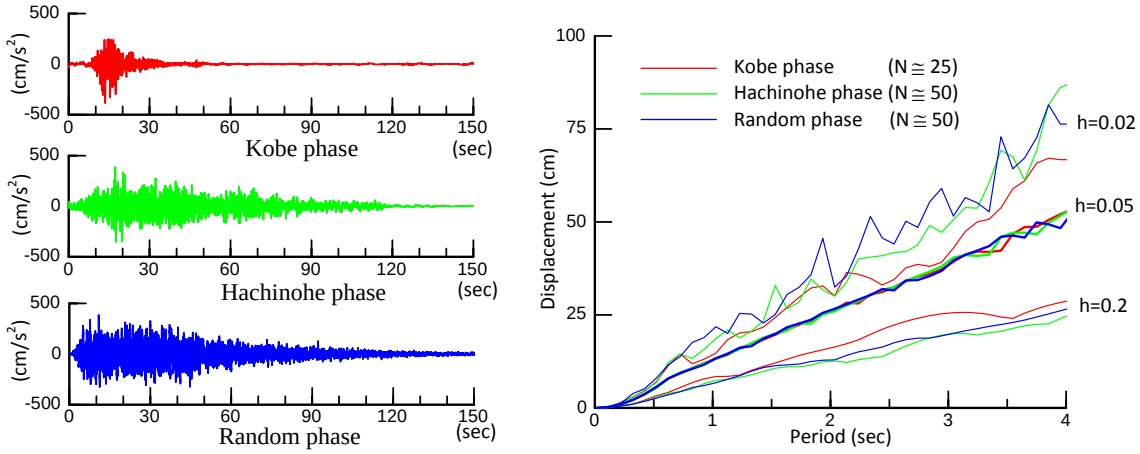

(a) Ground acceleration time history (b) Displacement response spectrum

Figure 11. Time history and velocity spectrum of input wave

Table 1. Model parameters

case	$\bar{e}_x$	$\bar{e}_y$	α_x	α_y	T (1st mode)	h_x	h_y
1	0	0	0.50	0.50	2.50*	0.05	0.05
2	0.371	0	0.50	0.54	2.82	0.05	0.05
3	0.742	0	0.50	1.00	3.40	0.05	0.086
4	0	0.223	0.50	0.50	2.64	0.05	0.05
5	0	0.446	0.69	0.50	2.93	0.05	0.05
6	0.371	0.223	0.50	0.54	2.91	0.05	0.05
7	0.742	0.446	0.69	1.00	3.61	0.05	0.086

* purely rotation mode

Fig. 12 shows the response analytical results. By setting the damper properties for each direction according to Eqns. 3.18 and 3.19, overall the response displacement of perimeter frames of the two-axis eccentric model is controlled within the response of conventional seismically designed structure for the X, Y and 45 degree inputs. It is also confirmed that the shear force, which is equivalent to absolute acceleration, is drastically reduced for the case with eccentricity. These results demonstrate the feasibility and effectiveness of the proposed DTS system.

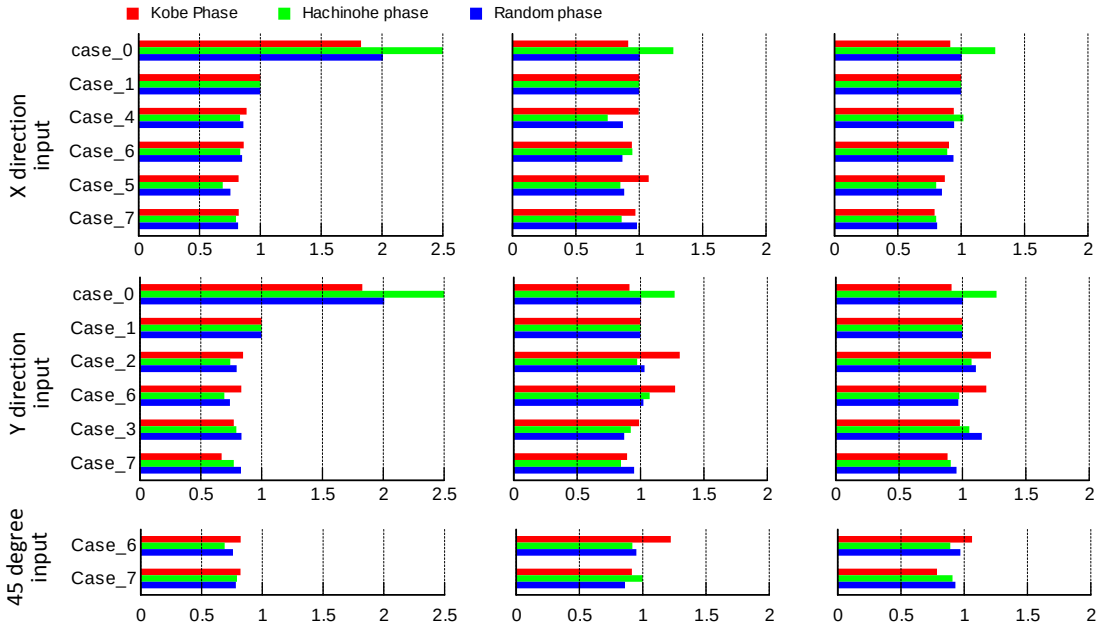

(a) Shear force (b) Displacement at point A (c) Displacement at point B

Figure 12. Earthquake response analysis result (normalized by response of Case_1)

5. CONCLUSIONS

This paper has proposed a new structural control system that realizes substantial earthquake response reduction utilizing torsional vibration, which is usually avoided in seismic design. This system consists of an eccentric core structure, flexible perimeter frames with pin-jointed post-columns that support only vertical loads, slab elements that transmit shear force between the core structure and the perimeter frames, and energy dissipation devices (dampers) installed in the perimeter frames. Inputted seismic energy is converted into torsional vibration energy due to the eccentricity of the core structure, and the dampers effectively absorb the energy. This system is nicknamed "Damper Tube Structure (DTS)". In addition to the attractive features for seismic design, the DTS has a possibility of realizing new architectural design in countries like Japan that are subject to severe earthquakes because the arrangement of the core is free and connections of other frames and slabs can be simple pin-jointed.

We first outlined the concept and the components of this system, and discussed the control effect and damper requirements including the optimum damper distribution problem using a simple one-axis eccentric mathematical model based on the CQC method and the viewpoint of energy balance. Then we proposed a simple design flow of the DTS including how to deal with the two-axis eccentric system, and conducted earthquake response analyses using a two-axis eccentric vibration model. The results are promising and the potential of the DTS was confirmed. Its applicability to high-rise buildings, cost performance, robustness of the control effect and a newly developed oil damper suitable for the DTS are to be discussed in another paper [Kano et al. 2012].

REFERENCES

Kano, N., Kurino, H., Tagami J. and Kaneko, T. (2012). Feasibility Study of Response Controlled Structurte with Eccentric Core and Damper Tube System. *15th World Conference on Earthquake Eingineeing.*